



Tenuibiotus yeliseii sp. nov., a new species of Macrobiotidae (Tardigrada: Eutardigrada) from Svalbard, Norway, with discussion of taxonomic criteria within the genus and its phylogeny

Tenuibiotus yeliseii sp. nov., новый вид из семейства Macrobiotidae (Tardigrada: Eutardigrada) с архипелага Шпицберген, Норвегия, с обсуждением таксономических критериев в рамках рода и его филогении

A.Yu. Tsvetkova & D.V. Tumanov

А.Ю. Цветкова, Д.В. Туманов

Alexandra Yu. Tsvetkova , Department of Invertebrate Zoology, Faculty of Biology, St Petersburg State University, 7/9 Universitetskaya Emb., St Petersburg 199034, Russia. E-mail: st072110@student.spbu.ru

Denis V. Tumanov , Department of Invertebrate Zoology, Faculty of Biology, St Petersburg State University, 7/9 Universitetskaya Emb., St Petersburg 199034, Russia; Zoological Institute, Russian Academy of Sciences, 1 Universitetskaya Emb., St Petersburg 199034, Russia. E-mail: d.tumanov@spbu.ru

Abstract. We describe *Tenuibiotus yeliseii* sp. nov., a new tardigrade species from Svalbard, using morphological and morphometric analyses conducted with the use of light and scanning electron microscopy, as well as genetic analyses based on four molecular markers (three nuclear, 18S rRNA, 28S rRNA, ITS-2, and one mitochondrial, COI). A phylogenetic analysis of the genus *Tenuibiotus* Pilato et Lisi, 2011 is conducted using new data. In addition, the taxonomic significance of gibbosities on legs IV as a key character for species identification in *Tenuibiotus* is discussed. A key to the species of *Tenuibiotus* is proposed.

Резюме. Описывается *Tenuibiotus yeliseii* sp. nov., новый вид тихоходок с архипелага Шпицберген, с использованием как морфологического и морфометрического анализа, выполненного с использованием световой и сканирующей электронной микроскопии, так и генетического анализа последовательностей четырёх молекулярных маркеров (трех ядерных: 18S рРНК, 28S рРНК, ITS-2, и одного митохондриального: COI). Приводятся результаты филогенетического анализа рода *Tenuibiotus* Pilato et Lisi, 2011 с учетом новых данных. Также обсуждается таксономическая значимость парных бугорков на четвёртой паре ног как ключевого признака для определения видов рода *Tenuibiotus*. Составлен ключ для определения видов *Tenuibiotus*.

Key words: Arctic, taxonomy, morphology, phylogeny, key, Tardigrada, Macrobiotidea, Macrobiotidae, *Tenuibiotus*, new species

Ключевые слова: Арктика, таксономия, морфология, филогения, ключ, Tardigrada, Macrobiotidea, Macrobiotidae, *Tenuibiotus*, новый вид

ZooBank Article LSID: 95922BF0-1BA0-4947-A23B-4C52B1F5703B

Introduction

Tardigrades are microscopic segmented animals known for their ability to withstand extreme con-

ditions in a cryptobiotic state. They inhabit aquatic biotopes from the abyssal depths of the ocean to mountain tops. The phylum currently comprises just over 1460 species (Degma & Guidetti, 2023).

In the recent years, investigations involving molecular data along with the traditional morphological approach have revealed unexpected diversity within most of the tardigrade taxa. Now the old paradigm of a wide distribution of polymorphic species has shifted, as newer investigations using a combined approach have revealed the presence of numerous local species that are poorly morphologically differentiated but clearly discernible using the methods of molecular taxonomy (Bertolani et al., 2011a; Gąsiorek et al., 2016, 2018; Stec et al., 2018; Guidetti et al., 2019).

A species group now known as the genus *Tenuibiotus* Pilato et Lisi, 2011 was initially isolated within the genus *Macrobiotus* Schultzze, 1834 as a *M. tenuis*-group by Maucci (1988). The group was named after *M. tenuis* Binda et Pilato, 1972 and was isolated on the basis of claw morphology and several other morphological characteristics. The *tenuis*-type claws are characterised by a longer common tract formed through fusion of the primary and secondary branches over a long distance.

Maucci (1988) included seven species in the *M. tenuis*-group: *M. ariekammensis* Węglarska, 1965, *M. higginsi* Maucci, 1987, *M. hyperonyx* Maucci, 1982, *M. hystricogenitus* Maucci, 1978, *M. mongolicus* Maucci, 1988, *M. tenuis* Binda et Pilato, 1972, and *M. willardi* Pilato, 1977.

The group was later discussed in two papers (Tumanov, 2005; Guil et al., 2007). Tumanov (2005) excluded *M. ariekammensis* from the *M. tenuis*-group and pointed out the phylogenetic insignificance of some characteristics suggested by Maucci. Guil et al. (2007) examined additional characters, but the *M. tenuis*-group still lacked a core definition.

Pilato & Lisi (2011) examined the holotypes of *M. tenuis* and *M. willardi*, and the paratypes of *M. ariekammensis*, *M. bondavallii* (Manicardi, 1989), *M. kirghizicus* (Tumanov, 2005), and *M. tenuiformis* (Tumanov, 2007). They considered the most substantial groups of characters (buccal apparatus and claw morphology), stating that the *tenuis*-type claw is a primary character with limited variability and high phyletic significance at the generic level. The authors therefore instituted a new genus *Tenuibiotus* that included species of the *tenuis*-group, mainly based on claw mor-

phology. Tumanov's (2005) suggestion to exclude species of the *M. ariekammensis* complex from the *M. tenuis*-group was supported by Pilato & Lisi (2011). In the recent publication by Stec et al. (2022), both species of the *M. ariekammensis* morphogroup were proved to belong to the genus *Macrobiotus* (s. str.) on the basis of the molecular phylogenetic analysis.

Following the integrative reexamination of *Tenuibiotus hyperonyx* by Stec & Morek (2022), this species was placed within the family Richtersiidae Guidetti et al., 2021, as *Diaforobiotus hyperonyx*. The authors additionally revised the genus and established another morphological diagnostic character, two macroplocoids in the pharynx, following the reexamination of *T. willardi* and *T. bozhkae* Pilato, Kiosya, Lisi, Inshina et Biserov, 2011, which resulted in a more comprehensive morphological diagnosis of *Tenuibiotus*.

It is also important to note that the recent large-scale phylogenies of Macrobiotidae or only Macrobiotidae superclade II have always recovered *Tenuibiotus* as a monophyletic taxon (Stec et al., 2021a; Kayastha et al., 2023).

The genus *Tenuibiotus* currently comprises 13 species: *T. bondavallii*, *T. bozhkae*, *T. ciprianoi* (Guil, Guidetti et Machordom, 2007), *T. danilovi* (Tumanov, 2007), *T. higginsi*, *T. hystricogenitus*, *T. kozharai* (Biserov, 1999), *T. mongolicus*, *T. tenuiformis*, *T. tenuis*, *T. voronkovi* (Tumanov, 2007), *T. willardi*, and *T. zandrae* Stec, Tumanov et Kristensen, 2020.

In this article, we describe a new species of the genus *Tenuibiotus* from Svalbard combining molecular techniques with classical morphometric and morphological methods in an integrative approach. In addition, we perform a phylogenetic analysis of *Tenuibiotus* using the new data, propose a key to the species of this genus, and discuss taxonomic significance of gibbosities on legs IV as a character for species identification in *Tenuibiotus*.

Material and methods

Sample processing. The moss and soil sample containing the new species was collected from the Svalbard Archipelago by Yelisei Mesentsev (St Petersburg State University) in 2019. The material was dried and stored in a paper envelope

at room temperature. Tardigrades were extracted from samples by soaking them overnight and washing through two sieves (Tumanov, 2018). The content of the fine sieve was examined under a Leica M205C stereomicroscope. All animals and eggs extracted from the sample were divided into three groups for further analysis: light microscopy [phase contrast (PhC) and differential interference contrast (DIC)], scanning electron microscopy (SEM) and DNA sequencing.

Microscopy and imaging. Specimens for light microscopy (LM) were fixed with acetic acid or relaxed by incubating live individuals at 60 °C for 30 min (Morek et al., 2016) and mounted on slides in Hoyer's medium. Permanent slides were examined under a Leica DM2500 microscope equipped with PhC and DIC, supplied with a Nikon DS-Fi3 digital camera with NIS software.

As preparation for SEM tardigrades were subjected to a 60 °C bath (Morek et al., 2016), then dehydrated in a series of water–ethanol mixtures (10%, 20%, 30%, 50%, 70%, 96% ethanol) and 100% acetone. The specimens then underwent CO₂ critical point drying, after which they were placed on stubs and sputter coated with a thin layer of gold (50 nm). Ultrastructural analysis of the body surface of the specimens was conducted under high vacuum in a Tescan MIRA3 LMU scanning electron microscope at the Centre for Molecular and Cell Technologies, St Petersburg State University.

All figures were assembled in Adobe InDesign CS4. For structures that could not be satisfactorily focused in a single LM photograph, a stack of 2–6 images was taken and assembled manually into a single deep-focus image, using Helicon Focus 6. Panorama Maker 6 was used to combine a series of images in cases where the entire structure did not fit into the camera field of view at high magnification.

Morphometrics and morphological terminology. Specimens were measured under LM using PhC. Sample size was adjusted following recommendations by Stec et al. (2016). All measurements are given in micrometers (µm). Structures were measured only if their orientation was suitable. Body length was measured from the anterior to the posterior end of the body, excluding the hind legs.

The terminology used to describe oral cavity armature follows Michalczyk & Kaczmarek (2003); claw morphology is described according to Pilato & Binda (2010). Macroplacoid length sequence is given according to Kaczmarek et al. (2014). Claws, elements of buccal apparatus, and egg shell structures were measured according to Kaczmarek & Michalczyk (2017). Cuticular structures under claws on legs 1–3 are described according to Kiosya et al. (2021). The *pt* index is the ratio of the length of a given structure to the length of the buccal tube expressed as a percentage (Pilato, 1981). Morphometric data were handled using ver. 1.6 of the “Parachela” template available from the Tardigrada Register (Michalczyk & Kaczmarek, 2013).

Genotyping. DNA was extracted from individual specimens using QuickExtract™ DNA Extraction Solution (Lucigen Corporation, USA; see description of complete protocol in Tumanov, 2020). Preserved exoskeletons were recovered, mounted on a microscope slide in Hoyer's medium and retained as the hologenophore (Pleijel et al., 2008).

Four genes were sequenced: the small ribosomal subunit (18S rRNA) gene, the large ribosomal subunit (28S rRNA) gene, the internal transcribed spacer (ITS-2) and the cytochrome oxidase subunit I (COI) gene. PCR reactions included 5 µl template DNA, 1 µl of each primer, 1 µl DNTP, 5 µl Taq Buffer (10×) (–Mg), 4 µl 25 mM MgCl₂ and 0.2 µl Taq DNA Polymerase (Thermo Scientific™) in a final volume of 50 µl. The primers and PCR programs used are listed in Electronic supplementary material 1 (see Addenda). The PCR products were visualised in 1.5% agarose gel stained with ethidium bromide. All amplicons were sequenced directly using the ABI PRISM Big Dye Terminator Cycle Sequencing Kit (Applied Biosystems) with the help of an ABI Prism 310 Genetic Analyzer in the Core Facilities Center “Centre for Molecular and Cell Technologies” of St Petersburg State University. Sequences were edited and assembled using ChromasPro software (Technelysium). The COI sequences were translated to amino acids using the invertebrate mitochondrial code, implemented in MEGA11 (Tamura et al., 2021), in order to check for the presence of stop codons and therefore of pseudogenes.

Comparative and phylogenetic molecular analyses. All sequences of 18S, 28S, ITS-2 and COI genes for the genus *Tenuibiotus* that were available in GenBank at the time of the analysis were downloaded. Sequences of appropriate length that were homologous to the sequences obtained and originated from publications with a reliable attribution of the investigated taxa were selected with addition of the newly obtained sequences (see Addenda: Electronic supplementary material 2). Uncorrected pairwise distances were calculated using MEGA11 with gaps/missing data treatment set to “pairwise deletion”. All obtained sequences were deposited in GenBank (<https://www.ncbi.nlm.nih.gov/genbank/>). 18S rRNA and 28S rRNA are nuclear markers used in phylogenetic analyses to investigate high taxonomic levels (Jørgensen et al., 2010, 2011; Guil & Giribet, 2012; Bertolani et al., 2014; Guil et al., 2019; Gąsiorek et al., 2019). COI is a protein-coding mitochondrial marker that is widely used as a standard barcode gene of intermediate to high effective mutation rate (Bertolani et al., 2011b). ITS-2 is a non-coding nuclear fragment with high evolution rates used for both intraspecific comparisons and comparisons between closely related species (Gąsiorek et al., 2016, 2018; Stec et al., 2018, 2021b). The sequences of *Mesobiotus anastasiae* Tumanov, 2020 of Macrobiotidae Thulin, 1928 were used as an outgroup, as it can be considered a representative species of the Macrobiotidae superclade I sensu Stec et al. (2021a) – with *Tenuibiotus*, *Paramacrobiotus* Guidetti, Schill, Bertolani, Dandekar et Wolf, 2009 and *Minibiotus* R.O. Schuster, 1980 belonging to superclade II.

Sequences were automatically aligned using the MAFFT algorithm (Katoh et al., 2002) using AliView version 1.27 (Larsson, 2014); the alignments were cropped to a length of 994 bp for 18S, 728 bp for 28S, 384 bp for ITS-2 and 654 bp for COI. Sequences of the four genes were concatenated using SeaView 4.0 (Gouy et al., 2010) (final alignment presented in Electronic supplementary material 3; see Addenda). The best substitution model and partitioning scheme for posterior phylogenetic analysis was chosen under the Akaike Information Criterion (AICc), using IQ-TREE multicore version 1.6.12 (Kalyaanamoorthy et al., 2017; Minh et al., 2020). IQ-TREE suggested re-

taining six predefined partitions separately. Models for each partition were chosen automatically (see Addenda: Electronic supplementary material 4). Maximum-likelihood (ML) topologies were constructed using IQ-TREE software (Minh et al., 2020) with appropriate models. Bayesian analysis of the same datasets was performed using MrBayes ver. 3.2.6, GTR model with gamma correction for intersite rate variation (8 categories) and the covariation model (Ronquist & Huelsenbeck, 2003). Analyses were run as two separate chains (default heating parameters) for 20 million generations, by which time they had ceased converging (final average standard deviation of the split frequencies was less than 0.01). The quality of chains was estimated using built-in MrBayes tools. MrBayes program was run at the CIPRES ver. 3.3 website (Miller et al., 2010). Bayesian analysis quality was verified using the program Tracer v1.7.1 (Rambaut et al., 2018).

Additional material examined. In scope of this study, we re-examined the type material of several species from the following collections (listed with abbreviations): BC – V. Biserov collection, University of Modena and Reggio Emilia; PBC – collection of G. Pilato and M.G. Binda, Catania University; RGC – R. Bertolani and R. Guidetti collection, University of Modena and Reggio Emilia; SPbU – Department of Invertebrate Zoology, Faculty of Biology, St Petersburg State University.

The types of the following species were re-examined: *T. bondavallii* (slide C990-S-23, paratype, RGC), *T. danilovi* [slides SPbU 190(9, 12), holotype and paratype, SPbU], *T. higginsi* (slide 12627, paratype, RGC), *T. kozharai* (slide 1540_9, holotype, BC), *T. mongolicus* (slides 12852, 12853, 12860, 12865, paratypes, RGC), *T. tenuiformis* [slides SPbU 197(11), 195(8, 21), 196(13), 197(12, 13, 16), 198(8), holotype and paratypes, SPbU], *T. tenuis* (paratype, PBC), *T. voronkovi* [slides SPbU 205(1, 2), holotype and paratype, SPbU]. In addition, the type specimens of *T. ciprianoi* (paratype, RGC) and *T. willardi* (RGC) were examined from the photos kindly provided by Roberto Bertolani and Giovanni Pilato.

The original descriptions of *T. hystricogenitus*, *T. bozhkae* and *T. zandrae* were used for comparison as well.

Results and discussion

Phylum **Tardigrada** Doyère, 1840

Class **Eutardigrada** Richters, 1926

Order **Parachela** Schuster, Nelson, Grigarick et Christenberry, 1980

Superfamily **Macrobitoidea** Thulin, 1928

Family **Macrobiotidae** Thulin, 1928

Genus ***Tenuibiotus*** Pilato et Lisi, 2011

***Tenuibiotus yeliseii* sp. nov.**

(Figs 1–5)

Holotype. Sex not determined; **Norway**, *Svalbard*, West Spitsbergen, nr. Longyearbyen settlm., 78°13'13.8"N 15°38'10"E; moss, leaf litter and soil, 15 Sept. 2019, Yelisei Mesentsev leg., SPbU 295(11).

Paratypes. Sex not determined; 8 adults and 20 eggs, same data as for holotype, SPbU 295(1, 2, 9–18, 27, 28, 32); 3 adults and 4 eggs, same data as for holotype, SEM stub, SPbU_Tar48.

The type specimens are kept at SPbU.

Morphological description. (Measurements and statistics in Table 1; see also Addenda: Electronic supplementary material 5). Body whitish, after mounting in Hoyer's medium transparent (Fig. 1a), with relatively short legs. Body surface with numerous well-developed cribose areas functioning as muscle attachment points (Fig. 1b). Eyes present in most of living specimens, visible after mounting. Body cuticle without pores; body surface with fine uniform sculpture consisting of minute granules visible under SEM only (Fig. 2a). Patches of dense granulation composed of cushions with aggregated granules present on all legs (Fig. 2b). Patches of granulation clearly visible under LM and SEM present on legs I–III on their outer surfaces and above claws (Fig. 4a, c). Inner surfaces of legs I–III lacking granulation (Fig. 4b); pulvinus absent. Patch of dense granulation present on legs IV, covering leg surface around claws (Fig. 4d, f, g).

Bucco-pharyngeal apparatus of *Macrobiotus*-type (Fig. 3a, i–k). Mouth anteroventral, surrounded by ten peribuccal lamellae. Oral cavity armature comprising three bands of teeth (Fig. 3b–h). Under LM, only second and third bands of teeth visible (second looking extremely faint) (Fig. 3e). However, under SEM all three bands of

teeth visible, with first band appearing as a narrow zone of very small teeth situated at bases of peribuccal lamellae (Fig. 3c). Second band of teeth situated posterior to ring fold of buccal cavity and represented by a wider zone of larger granular or cone-shaped teeth (Fig. 3d, e). Third band of teeth divided into three dorsal and three ventral transverse ridges. Dorsomedial ridge slightly caudally curved (Fig. 3d, f); ventromedial ridge apparently consisting of closely spaced and partially fused large teeth (Fig. 3g). (Granular structures posterior to third band of teeth visible in LM images identified as food particles in buccal cavity.)

Stylet furcae with well-developed spherical condyles (Fig. 3i). Ventral lamina relatively long, constituting more than half of length of buccal tube (Fig. 3i). Buccal tube terminating in well-developed apophyses (Fig. 3j, k). Pharyngeal bulb containing two elongate macroplacoids and a drop-like microplacoid. Macroplacoid length sequence $2 < 1$. First macroplacoid with central constriction whereas second macroplacoid constricted subterminally (Fig. 3j, k).

Claws of *tenuis*-type, large, primary branches with distinct accessory points (Fig. 4a, c, d, g). Lunulae large on all legs, especially on legs IV. Lunulae I–III smooth (Fig. 4a, c), lunulae IV with clear dentation (Fig. 4d, f, g). Legs I–III only with double muscle attachments under claws, without cuticular bars (Fig. 4e). Lunulae on legs IV connected by a horseshoe structure visible under LM (Fig. 4f). Each hind leg with a pair of gibbosities on dorsal surface, right above claws (Fig. 4d, f, g).

Eggs (measurements and statistics in Table 2; see also Addenda: Electronic supplementary material 5). Laid freely, yellow whitish, spherical, with relatively small conical processes (Fig. 5a–d). Apices of processes often furcated, sometimes bent towards egg surface (Fig. 5f). Several rows of roundish pores visible only under SEM on basal surface of processes (Fig. 5f), with pores not fully perforating the process wall and instead appearing as individual round recesses (Fig. 5g). Apical surface without pores. Surface between processes lacking areolation or reticulation but bearing minute sparsely spaced pores and system of well-developed radial ridges, visible under SEM (Fig. 5e, f: incut). Layered egg chorion with pillars (Fig. 5g) appearing as dots on egg surface under LM (Fig. 5e).

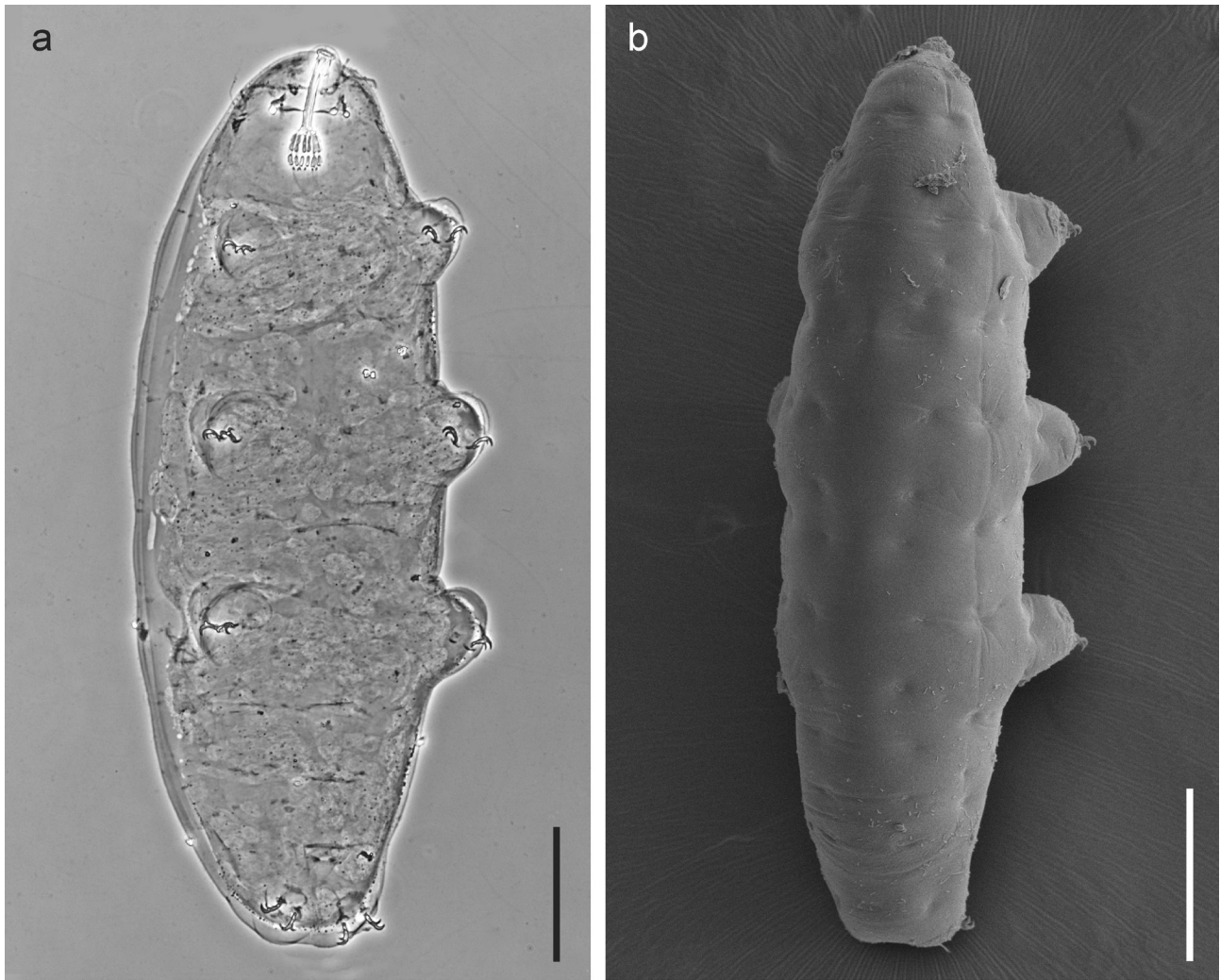


Fig. 1. *Tenuibiotus yeliseii* sp. nov., habitus. **a**, dorsoventral view (holotype, PhC); **b**, dorsal view (paratype SPbU_48, SEM). Scale bars: 100 μ m.

Of all the eggs discovered, several contained fully formed embryos. The claw shape and placoid configuration of the embryos matched those in adult specimens. Moreover, all other species found in the same sample belong to the superfamily Hypsibioidea; they are characterised by laying their eggs into exuviae after molting. Therefore, we can conclude that all discovered eggs belong to the new species.

Phenotypic comparison. *Tenuibiotus yeliseii* sp. nov. is most similar to *T. voronkovi* also known from Svalbard (Tumanov, 2007; not *T. voronkovi* sensu Zawierucha et al., 2016; see also Stec et al., 2020), but is easily distinguished from it by the structure of egg processes (by the presence of rows of pores at the bases of processes), and by the ab-

sence of granulation on the dorsal and lateral body cuticle visible under LM.

Compared to the other *Tenuibiotus* species, *T. yeliseii* sp. nov. differs from *T. bondavallii* [described from Canada by Manicardi (1989) and later reported from Russia, namely, from Dikson Island, the Taimyr Peninsula (Biserov, 1996) and the Kuril Islands (Dudichev & Biserov, 2000), but the records from Russia need verification] in the absence of granulation on the dorsal body cuticle in the posterior region visible under LM [vs. body surface sculpture visible under LM (Fig. 8a)] and in much smaller egg processes (process base diameter ranging 7.7–13.4 μ m in *T. yeliseii* sp. nov., while process base diameter in *T. bondavallii* is measured to be 16–18 μ m);

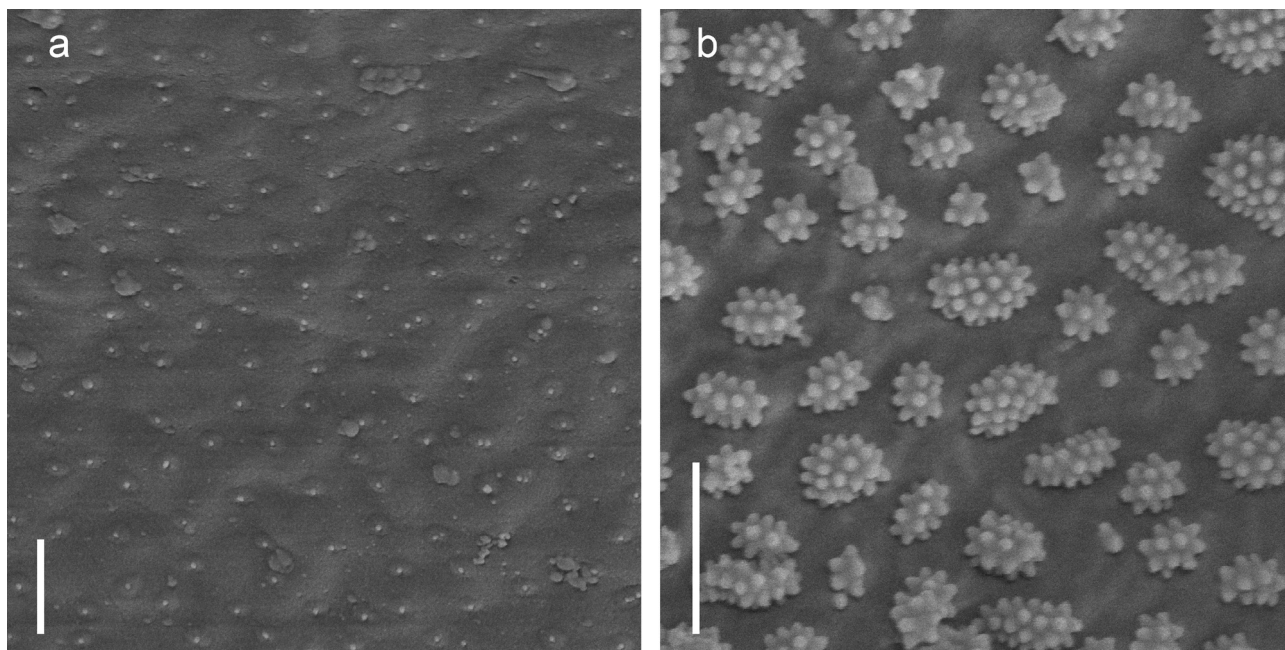


Fig. 2. *Tenuibiotus yeliseii* sp. nov., cuticular sculpture (paratype SPbU_48, SEM). **a**, body surface sculpture (minute granules); **b**, leg granulation. Scale bars: 1 μ m.

from *T. bozhkae* [described from the Crimean Peninsula by Pilato et al. (2011)], in the larger eggs (87 μ m bare diameter / 123 μ m diameter with processes in *T. bozhkae* vs. 116/138 μ m on average in the new species) and in wider process bases (6.1–6.3 μ m in *T. bozhkae*, with the processes therefore appearing more narrow and elongate, vs. 7.7–13.4 μ m in the new species);

from *T. ciprianoi* [described from Spain by Guil et al. (2007)], in the presence of well-developed accessory points on the main claw branch, in narrower and more elongate macroplacoids, and in wider egg processes (process height / base width ratio ranging 120–286% in *T. ciprianoi* vs. 50–110% in the new species);

from *T. danilovi* [known from Kyrgyzstan (Tumanov, 2007; Stec et al., 2021)], in the shape of mediodorsal ridge of buccal armature (paired granules in *T. danilovi* and arch-shaped ridge in the new species) and in larger egg processes (30 on the egg circumference in *T. danilovi* vs. only 20–23 in the new species);

from *T. higginsi* [described from Wyoming, USA, by Maucci (1987)], in the significantly shorter claws, especially on legs IV (length of claws on hind legs up to 28 μ m in *T. higginsi* vs. 9.2–16.8 μ m in the new species; with *pt* index for

claws on hind legs 41.2 in the holotype of *T. higginsi** vs. *pt* range 24.2–31.4 in the new species) and in narrower and taller egg processes (process height / base width ratio is 40% in *T. higginsi* vs. 50–110% in the new species);

from *T. hystricogenitus* [described from Turkey (Maucci, 1978), later recorded from Germany and Greece (McInnes, 1994); the record from Alaska (Johansson et al., 2013) needs verification (Kaczmarek et al., 2016)], in the shape of egg processes (filiform and flexible in *T. hystricogenitus* vs. conical in the new species);

from *T. kozharai* [described from Turkmenistan by Biserov (1999)], in the well-pronounced accessory points and in a longer ventral lamina (less than half of the buccal tube length in *T. kozharai* vs. 52.0–59.4% of its length in the new species);

from *T. mongolicus* [described from Mongolia by Maucci (1988)], in the narrower buccal tube (mean *pt* index for internal width is 11.05 ± 1.37 in *T. mongolicus* vs. 6.8 ± 1.1 in the new species);

* We calculated the *pt* index from the measurements provided in the original description of *T. higginsi* (Maucci, 1987).

Table 1. Summary of morphometric data for *Tenuibiotus yeliseii sp. nov.*

Character	n	Range		Mean		SD		Holotype	
		µm	pt	µm	pt	µm	pt	µm	pt
Body length	7	291–654	871–1167	500	1020	131	104	654	1135
Buccopharyngeal tube									
Buccal tube length	9	33.4–57.6	–	49.8	–	8.5	–	57.6	–
Stylet support insertion point	9	24.6–43.9	71.5–76.2	37.3	74.8	6.5	1.5	43.9	76.2
Buccal tube external width	9	3.3–6.9	9.7–12.2	5.5	11.0	1.2	0.9	6.3	11.0
Buccal tube internal width	9	2.0–4.9	5.6–9.1	3.4	6.8	1.0	1.2	4.3	7.5
Ventral lamina length	9	17.4–32.3	52.0–59.4	27.4	54.9	5.2	2.6	31.0	53.8
Placoid lengths									
Macroplacoid 1	9	6.7–13.6	20.1–25.0	11.2	22.3	2.3	1.8	12.7	22.0
Macroplacoid 2	9	3.6–8.4	10.8–14.9	6.7	13.3	1.6	1.4	7.6	13.1
Microplacoid	9	1.2–2.5	3.5–4.4	1.9	3.8	0.4	0.3	2.2	3.9
Macroplacoid row	9	11.8–24.3	35.3–44.7	19.8	39.5	4.2	2.6	22.8	39.5
Placoid row	9	13.8–27.1	41.3–49.7	22.6	45.0	4.7	2.5	26.3	45.7
Claw 1 lengths									
External primary branch	9	8.5–15.3	22.2–27.3	12.3	24.6	2.5	1.6	13.5	23.5
External secondary branch	9	6.5–12.4	16.9–22.2	9.7	19.4	2.1	1.6	10.3	17.8
Internal primary branch	9	8.4–14.2	21.7–27.6	11.9	23.9	2.1	1.9	13.6	23.5
Internal secondary branch	9	6.2–11.1	14.2–19.9	8.8	17.7	1.9	1.9	9.9	17.1
Claw 2 lengths									
External primary branch	9	8.9–17.9	23.7–32.0	13.2	26.5	2.9	2.4	14.9	25.9
External secondary branch	9	6.8–15.0	18.5–26.9	10.4	20.7	2.5	2.5	11.7	20.4
Internal primary branch	8	9.0–16.8	23.1–30.1	12.8	25.6	2.7	2.2	13.8	24.0
Internal secondary branch	8	7.1–13.7	15.3–24.5	9.7	19.4	2.3	2.7	10.2	17.7
Claw 3 lengths									
External primary branch	6	8.8–14.7	22.7–26.3	11.8	25.1	2.6	1.4	?	?
External secondary branch	6	6.1–11.1	18.2–20.4	9.1	19.3	2.0	0.9	?	?
Internal primary branch	5	8.3–13.1	22.9–24.8	11.5	23.8	2.0	0.8	?	?
Internal secondary branch	5	6.3–10.0	16.4–18.7	8.5	17.7	1.5	0.9	?	?
Claw 4 lengths									
Anterior primary branch	8	8.5–17.2	25.5–29.8	13.6	27.6	3.0	1.5	17.2	29.8
Anterior secondary branch	8	6.2–12.4	17.9–22.8	9.8	19.8	2.3	1.7	12.4	21.5
Posterior primary branch	8	9.2–16.8	24.2–31.4	13.6	27.7	2.9	2.0	16.1	28.0
Posterior secondary branch	8	6.8–12.5	17.6–23.2	10.3	20.8	2.3	1.6	12.3	21.4

Notes. Measurements are given in µm, *pt* values in % (*pt* index is a percentage ratio between the length of a structure and the length of the buccal tube). SD – standard deviation.

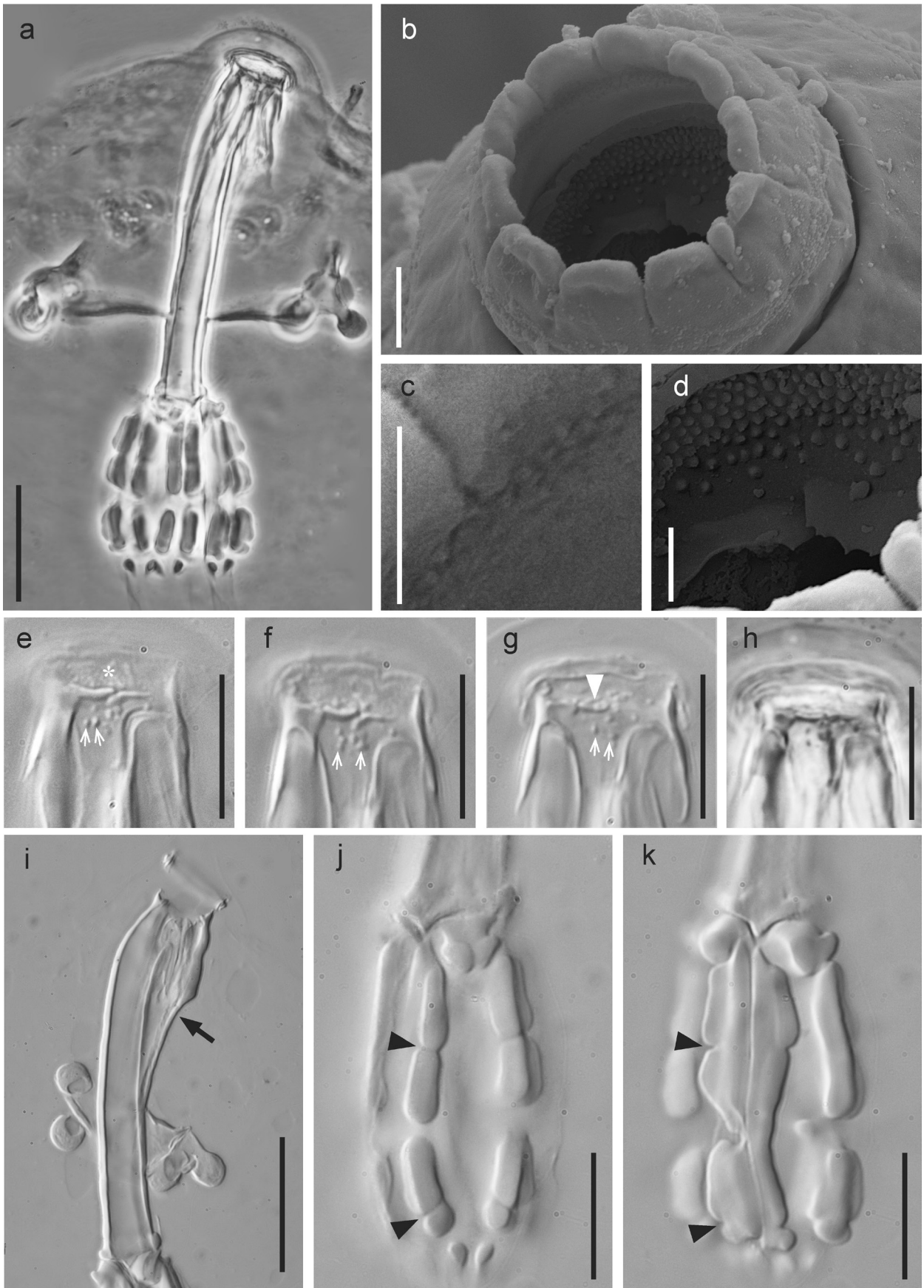


Table 2. Summary of morphometric data for eggs of *Tenuibiotus yeliseii* sp. nov.

Character	n	Range	Mean	SD
Egg bare diameter	5	104.4–126.1	116.7	8.8
Egg full diameter	5	134.0–146.1	138.5	5.3
Process height	47	8.7–20.7	14.2	2.7
Process base width	47	7.7–13.4	9.9	1.3
Process base/height ratio	47	50–110%	72%	13%
Inter-process distance	57	0.4–3.8	1.7	0.8
Number of processes on the egg circumference	5	20–23	22	1.4

Notes. Measurements are given in μm . N – number of eggs/structures measured, range refers to the smallest and the largest structure among all measured specimens; SD – standard deviation.

from *T. tenuiformis* [described from Kyrgyzstan (Tumanov, 2007; Stec et al., 2021) and also reported from China (Beasley & Miller, 2012)], in the absence of a large mediodorsal tooth in the buccal armature, in the shape of egg processes (truncated cones in *T. tenuiformis* vs. elongate cones in the new species);

from *T. tenuis* [described from Italy by Binda & Pilato (1972); Canadian record needs verification (Kaczmarek et al., 2016)], in the shape of egg processes (truncated cones in *T. tenuis* vs. elongate cones in the new species);

from *T. willardi* [described from Canada (Pilato, 1977), also reported from USA, Greenland, Poland and numerous locations in Russia (McInnes, 1994; Kaczmarek et al., 2016)], in the presence of well-pronounced teeth on leg 4 lunules and in the size of the eggs (bare diameter ranging 74–82 μm in *T. willardi* vs. 104.4–126.1 μm in the new species);

from *T. zandrae* [described from Greenland (Stec, Tumanov et Kristensen, 2020)], in the absence of granulation on the dorsal body cuticle

visible under LM, in the absence of granulation on the inner surfaces of legs I–III, in well-developed medioventral ridge with less pronounced fragmentation, the presence of rows of roundish pores at the base of egg processes (such pores completely absent in *T. zandrae*), in a larger number of these processes (13–15 processes on the egg circumference in *T. zandrae* vs. 20–24 in the new species) and in smaller size of the processes (process base width ranging 13.6–29.6 μm in *T. zandrae* vs. 7.7–13.4 μm in the new species).

DNA sequences. Sequences of good quality for the four molecular markers mentioned above were obtained from three paratypes [two hologenophores available: voucher specimens 295(1) and 295(2)], except for the ITS-2 marker, which was obtained from two specimens only. Each gene was represented by a single haplotype. All obtained sequences were deposited in GenBank.

18S rRNA sequence (GenBank: OR142418–OR142420), 1011, 1033 and 1008 bp long.

28S rRNA sequence (GenBank: OR142426 – OR142428), 729, 736 and 732 bp long.

Fig. 3. *Tenuibiotus yeliseii* sp. nov., bucco-pharyngeal apparatus [a, e–h, holotype; b–d, paratype SPbU_48; i–k, paratype SPbU 295(1)]. **a**, total dorsoventral view of bucco-pharyngeal apparatus (PhC); **b**, oral cavity with peribuccal lamellae (SEM); **c**, **d**, buccal armature (c, first row of teeth; d, the second and third rows of teeth, dorsal side; SEM); **e–g**, oral cavity armature, middle view with the second band of teeth (e), dorsal (f) and ventral (g) view of the third band of teeth (DIC; white arrows indicate food particles in the buccal cavity; e, the second band of teeth marked by asterisk; g, medioventral tooth indicated by white arrowhead); **h**, dorsal buccal armature (PhC); **i**, side view of buccal tube (DIC; black arrow points to ventral lamina); **j**, **k**, placoid configuration in pharynx (j, lateral rows of placoids; k, medial row of placoids; DIC; black arrowheads indicate constrictions on macroplacoids). Scale bars: a, i – 20 μm , b – 2 μm , c, d – 1 μm , e–g, j, k – 10 μm , h – 5 μm .

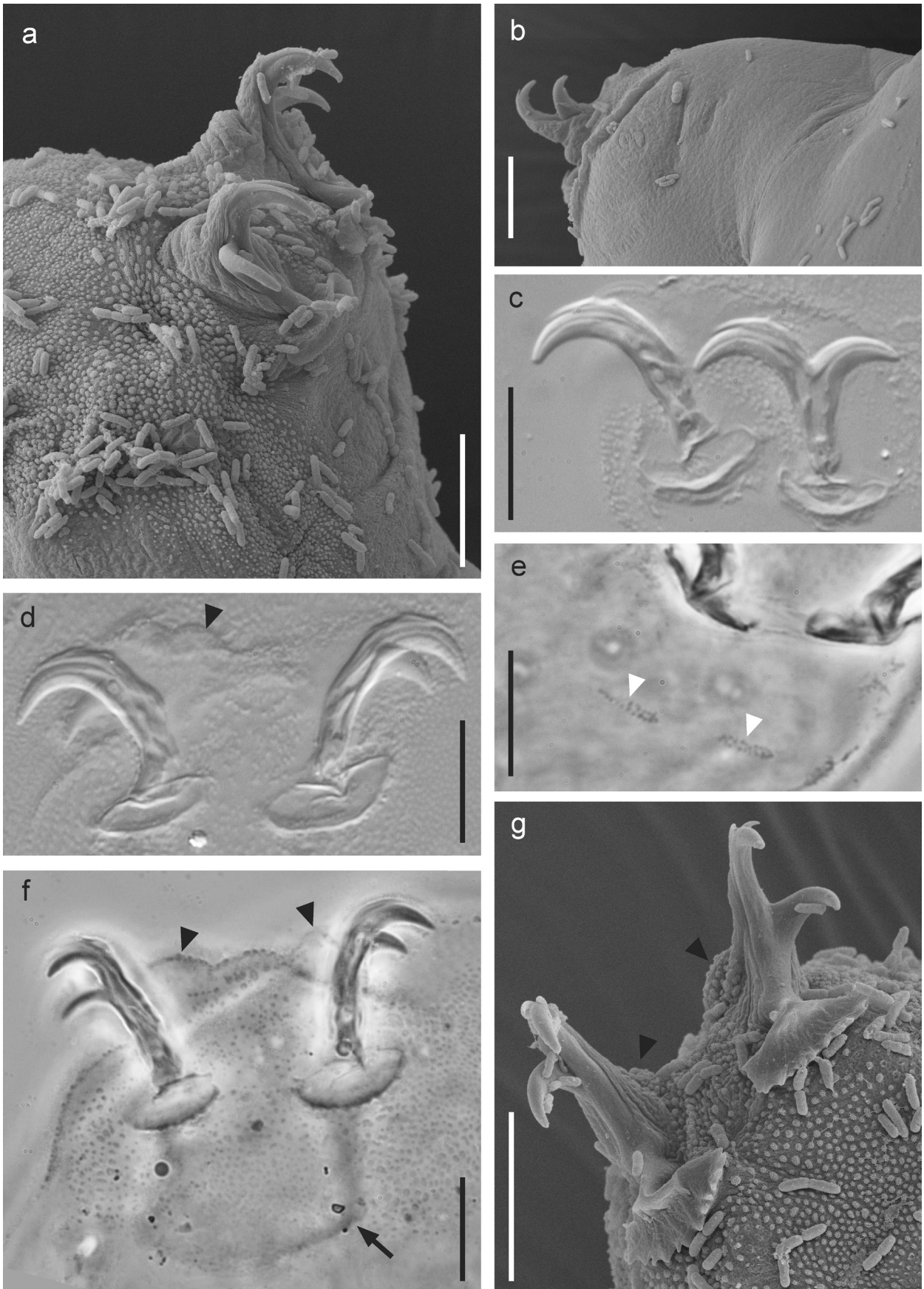


Fig. 4. *Tenuibiotus yeliseii* sp. nov., legs [a, b, g, paratype SPbU_48; c, d, paratype SPbU (295(9)); e, f, holotype]. **a**, outer surface of leg II with developed granulation (SEM); **b**, inner surface of leg II without granulation (SEM); **c**, claws on leg II (DIC); **d**, claws on leg IV (DIC); **e**, claws on leg I (PhC); **f**, claws on leg IV (PhC); **g**, claws on leg IV (SEM). Black arrowheads (d, f, g) indicate paired gibbosities on hind legs; white arrowheads (e) indicate muscle attachment points below the lunules; black arrow (f) marks the horseshoe structure connecting the lunules. Scale bars: 10 μ m.

ITS-2 sequence (GenBank: OR142424 and OR142425), 370 and 422 bp long.

COI sequence (GenBank: OR145334–OR145336), 681, 699 and 696 bp long.

Molecular comparison. The ranges of uncorrected genetic p -distances between the studied population of *Tenuibiotus yeliseii* sp. nov. and the other species of the genus *Tenuibiotus*, for which sequences were available from GenBank (see Addenda: Electronic supplementary material 2) are as follows:

18S rRNA: our analysis shows that all examined species of *Tenuibiotus* do not differ by the 18S rRNA fragment chosen for calculating p -distances, therefore appearing to share the same haplotype.

28S rRNA: 0.28%–4.18% (mean 1.76%), with the most similar being *T. zandrae* (Stec et al., 2020) from Greenland (MN443035: Stec et al., 2020), and the least similar being *T. tenuiformis* from Kyrgyzstan (MN888363: Stec et al., 2021).

ITS-2: 0.54%–12.30% (mean 4.50%), with the most similar being *T. aff. voronkovi** from Nordaustlandet (KX810046–KX810048: Zawierucha et al., 2016), and the least similar being *T. tenuiformis* (MN888350: Stec et al., 2021).

COI: 12.43%–24.75% (mean 17.95%), with the most similar being *T. aff. voronkovi* from Nordaustlandet (KX810043: Zawierucha et al., 2016), and the least similar being *T. tenuiformis* (MN888330: Stec et al., 2021).

* The sequences of *T. aff. voronkovi* used in the analysis were presented in a study of Zawierucha et al. (2016). The authors provided a redescription of *T. voronkovi*, adding the molecular data to the existing morphological description. However, Stec et al. (2020) reexamined the material used by Zawierucha et al. and concluded that it significantly differs morphologically from the type material collected by Tumanov (2007). Therefore *T. aff. voronkovi* is most likely a yet undescribed *Tenuibiotus* species, which closely resembles *T. zandrae* (see discussion in Stec et al., 2020).

Full matrices with p -distances are provided in Electronic supplementary material 6.

Etymology. We dedicate the new species to Yelisei Mesentsev, who kindly collected the samples on the Svalbard Archipelago during an expedition in 2019.

Phylogenetic analysis

Both analyses resulted in the trees with almost identical topology. Bayesian tree was used as a base (Fig. 6). The new species described in this study clusters together with two other *Tenuibiotus* taxa (*T. zandrae* and *T. aff. voronkovi*) from arctic territories in a well-supported species group.

Our multilocus phylogeny reconstruction demonstrates that for the arctic territories the geographical distribution closely matches the genetic relationships within the species group. As both previously described species are from Greenland (*T. zandrae*) and Svalbard (*T. aff. voronkovi*), and the new species is also described from Svalbard, the presence of a well-supported clade containing these three taxa may indicate an intense Tardigrada speciation process in the Arctic.

Several branches remain unresolved due to the significant lack of molecular data available for the genus *Tenuibiotus*. Further investigation is required, as well as collecting the genetic information on previously morphologically described species.

The significance of gibbosities on legs IV as a character for species identification in *Tenuibiotus*

The presence of two small gibbosities near the claws on legs IV was introduced as an additional significant character in the morphological diagnosis of *T. bozhkae* (Pilato et al., 2011). During our investigation, original slides in our collection were examined, as well as photographs and slides from

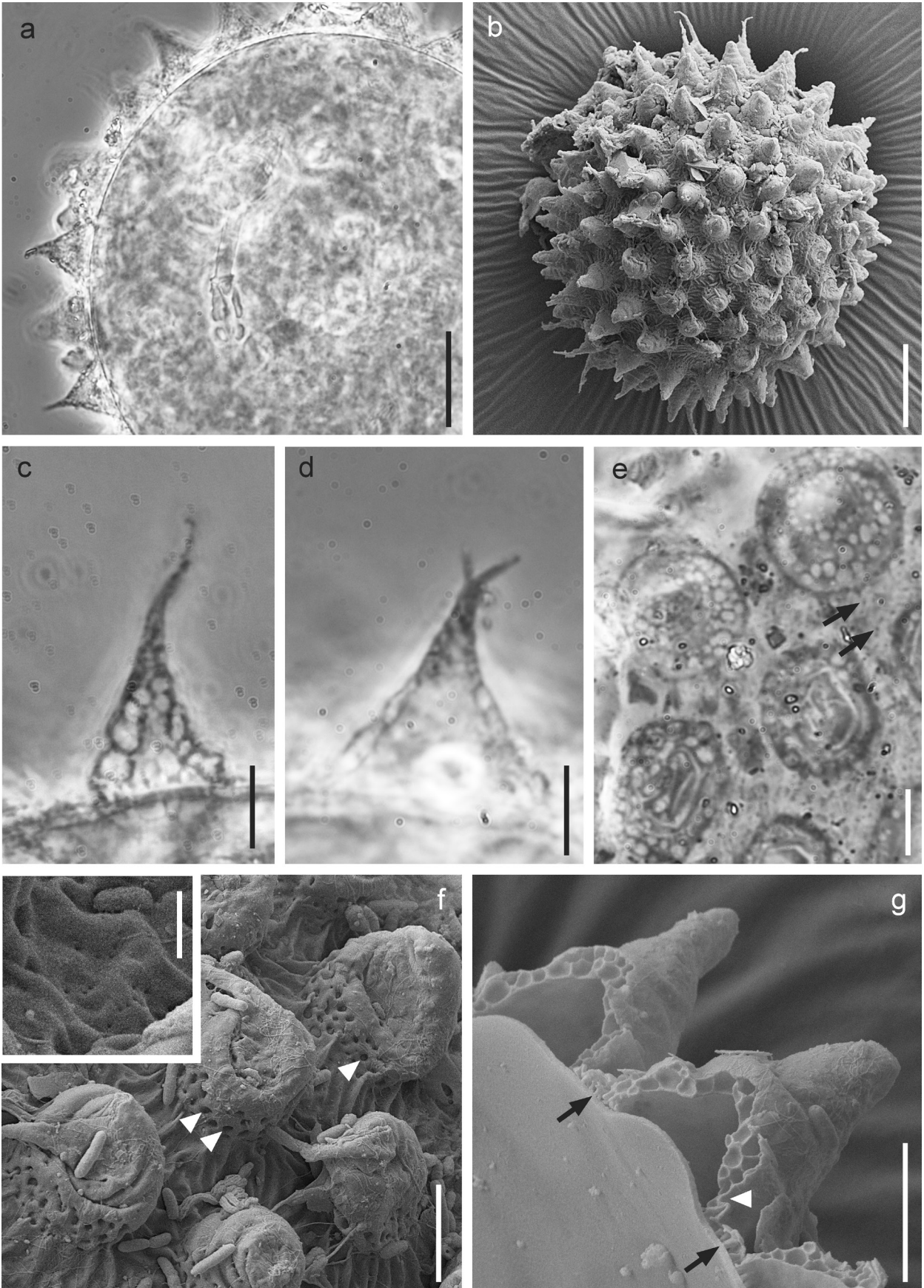


Fig. 5. *Tenuibiotus yeliseii* sp. nov., egg chorion morphology [paratypes: a, d, SPbU (295(12)); b, f, g, SPbU_48; c, SPbU (295(16)); e, SPbU (295(13))]. **a**, midsection (fragment; PhC); **b**, entire egg (SEM); **c**, **d**, midsections of processes of two different eggs (PhC); **e**, egg surface between the processes (PhC); **f**, egg surface at higher magnification (incut: pores in the egg surface; SEM); **g**, fractured chorion, details of process wall structure (SEM). White arrowheads indicate the pores on the basal surface of processes, black arrows point to the pillars in the egg chorion, visible as dots under LM. Scale bars: a, b – 20 µm, c–g – 5 µm, incut – 1 µm.

the collections of our colleagues (see Additional material for details). We discovered that this feature is not unique to *T. bozhkae*. Of all thirteen currently described species of the genus *Tenuibiotus*, nine possess a pair of gibbosities on the dorsal surface of the hind legs, directly above the claws. These species are *T. bondavallii*, *T. bozhkae*, *T. danilovi*, *T. higginsii*, *T. kozharai*, *T. mongolicus*, *T. tenuiformis*, *T. tenuis* (six of them are illustrated in Fig. 7) and *T. zandrae* (Stec et al., 2020: 18, Fig. 14B). Moreover, the paired gibbosities are also present in the new species, making the ratio 10/14.

We could not prove the presence or the absence of these structures in *T. ciprianoi* (description lacking details; type material not examined), *T. hystricogenitus* (character not mentioned; type material not examined), *T. voronkovi* (damaged hind legs in the type material) and *T. willardi* (description lacking details; type material not examined). Nevertheless, the remaining ten species sharing this character render it meaningless for the identification of any particular species in the genus *Tenuibiotus*. We therefore propose that the character of possessing paired gibbosities on legs IV

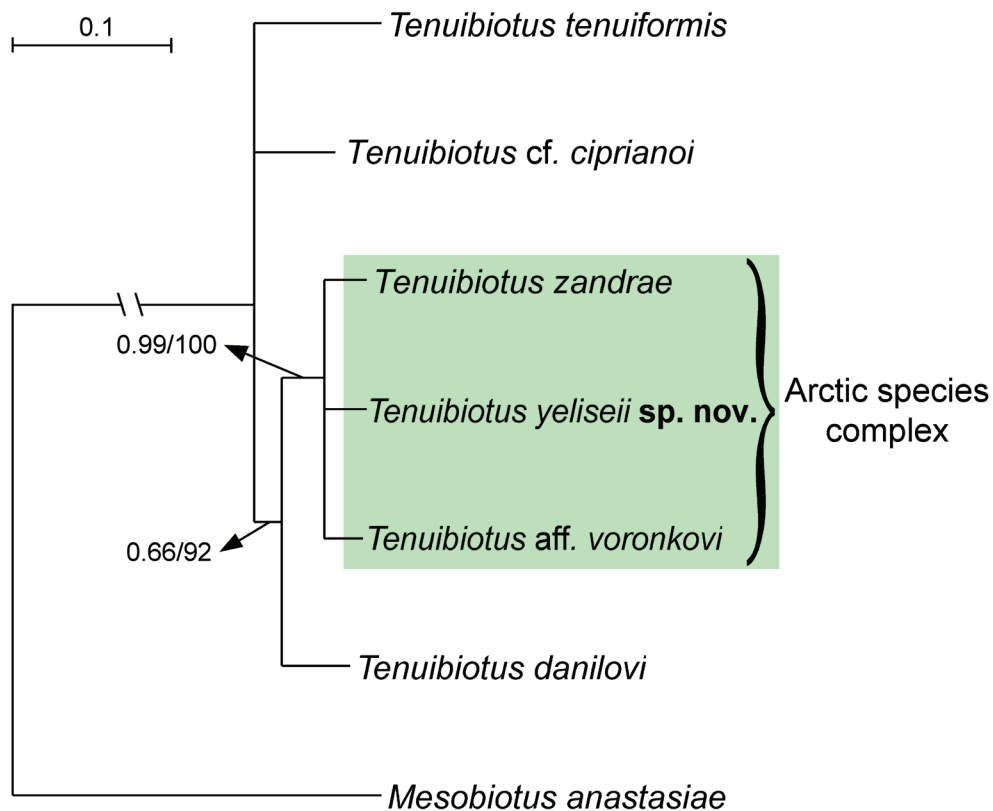


Fig. 6. Phylogeny of the genus *Tenuibiotus* based on concatenated 18S rRNA, 28S rRNA, ITS-2 and COI sequences. Numbers at nodes indicate Bayesian posterior probability values (BI, first values) and bootstrap values (ML, second values). Branches with support below 0.9 in BI and below 70% in ML were collapsed. Scale bar and branch lengths refer to the Bayesian analysis.

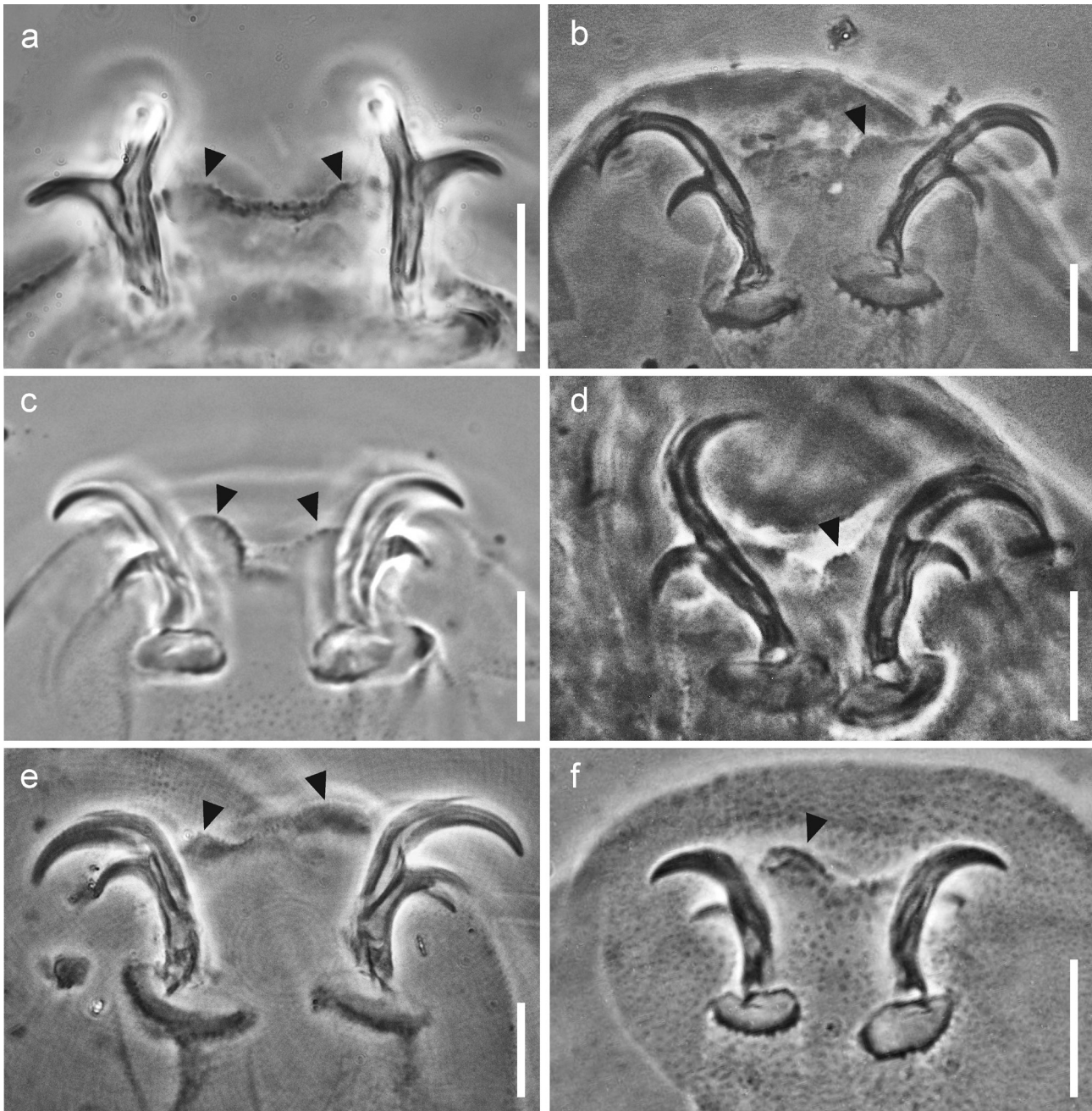


Fig. 7. *Tenuibiotus* spp., paired gibbosities (indicated by arrowheads) on hind legs (PhC). **a.** *T. danilovi* (Tumanov, 2007) [paratype SPbU 190(13) at SPbU]; **b.** *T. higginsii* (Maucci, 1987) (paratype 12627 at PBC); **c.** *T. kozharai* (Biserov, 1999) (holotype at BC); **d.** *T. mongolicus* (Maucci, 1988) (paratype 12853 at RGC); **e.** *T. tenuiformis* (Tumanov, 2007) [paratype SPbU 195(8) at SPbU]; **f.** *T. tenuis* (Binda et Pilato, 1972) (paratype at PBC). Scale bars: 10 μ m.

has no significance in the morphological diagnosis of *T. bozhkae*.

It is also important to note that the visibility of the gibbosities seems to depend on the orientation of the specimen, even under SEM, as evidenced by the illustrative material for *T. zandrae* (Fig. 14D

in the original description). More interestingly, these images also suggest the presence of similar structures on other pairs of legs (Fig. 14C in the original description). Moreover, the distribution of these gibbosities across the Macrobiotidae is still an open question.

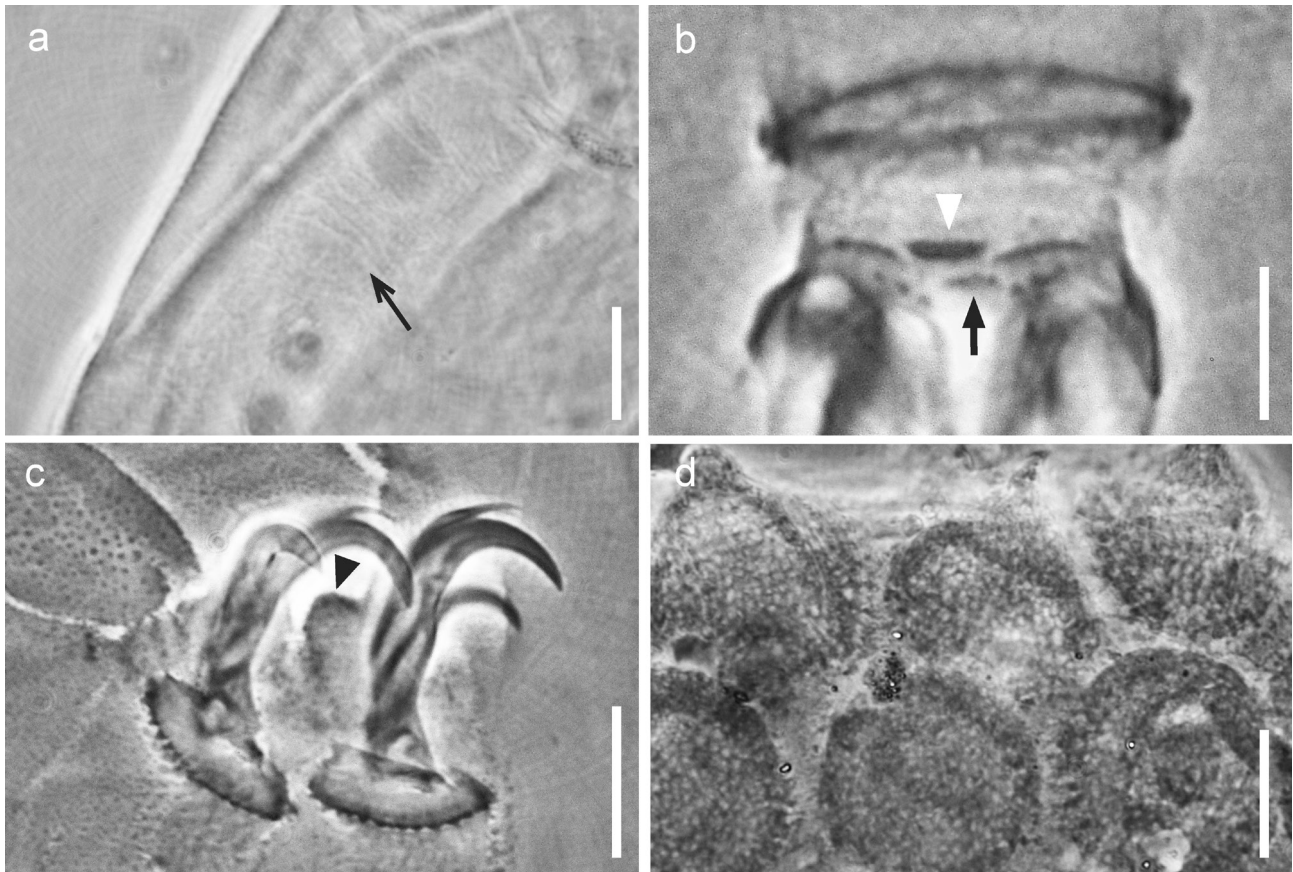


Fig. 8. *Tenuibiotus bondavallii* (Manicardi, 1989) (paratype C990-S-23 at PBC; PhC). **a**, cuticular sculpture on the caudal region (indicated by a black simple arrow); **b**, buccal armature (white arrowhead points to the medio-dorsal ridge, black triangular arrow indicates the medioventral ridge); **c**, claws on leg IV (black arrowhead points to the gibbosity dorsal to the claw); **d**, surface of the egg chorion. Scale bars: a, c, d – 10 μ m, b – 5 μ m.

Key to the species of the genus *Tenuibiotus*

- | | |
|--|---------------------------|
| 1. Egg processes long, thin, filiform | <i>T. hystricogenitus</i> |
| – Egg processes of another shape 2 | |
| 2. Egg processes conical, truncated 3 | |
| – Egg processes conical with pointed ends 4 | |
| 3. Dorsal buccal armature (under LM) in the shape of a single triangular crest pointing backwards | <i>T. tenuiformis</i> |
| – Dorsal buccal armature (under LM) with transverse ridges | <i>T. tenuis</i> |
| 4. Dorsal buccal armature consists of two large separate granules | <i>T. danilovi</i> |
| – Dorsal buccal armature of another configuration 5 | |
| 5. Granulation visible under LM present on the dorsal side of body 6 | |
| – Granulation visible under LM absent on the dorsal body cuticle 8 | |
| 6. Number of processes on egg circumference more than 20 | <i>T. voronkovi</i> |
| – Number of processes on egg circumference no more than 15 7 | |
| 7. Mediodorsal ridge of the buccal armature in shape of a triangular tooth pointed backwards; medioventral ridge appears as separate granules; cuticular sculpture on the dorsal and ventral sides of the body visible under LM as distinct dotted pattern | <i>T. zandrae</i> |
| – Mediodorsal ridge in shape of a transverse line; medioventral ridge undivided; cuticular sculpture only on the caudal dorsum visible under LM as indistinct granulation (Fig. 8a) | <i>T. bondavallii</i> * |

* In the 2020 paper describing *T. zandrae*, Stec et al. used one character for differentiating between the new species and *T. bondavallii*: the areolation around the bases of the egg processes, present in *T. bondavallii* but absent in *T. zandrae*. However, those areoles are only present in illustrations in the original description of *T. bondavallii* made by Manicardi in 1989, who did

8. Claws with poorly developed accessory points, almost indiscernible under LM 9
- Claws with well-developed accessory points 10
9. Egg process height under 10 µm (5–9 µm) *T. kozharai*
- Egg process height over 10 µm (12–20 µm). *T. ciprianoi*
10. Egg processes short (height-to-width ratio under 50%), with blunt apices. *T. higginsi*
- Egg processes elongated (height-to-width ratio over 50%) 11
11. Egg process height-to-width ratio 250–350% .. 12
- Egg process height-to-width ratio 50–200%. 13
12. Buccal tube external width *pt* index over 15. *T. willardi*
- Buccal tube external width *pt* index under 12. *T. bozhkae*
13. Buccal tube internal width *pt* index over 10. *T. mongolicus*
- Buccal tube internal width *pt* index under 10. *T. yeliseii* sp. nov.

Addenda

Electronic supplementary material 1. Primers and PCR programs used for amplification of four DNA fragments sequenced in the study. File format: PDF.

Electronic supplementary material 2. Complete list of sequences used in the molecular phylogenetic analysis. File format: PDF.

Electronic supplementary material 3. Final alignment used for the phylogenetic analyses. File format: Fasta.

Electronic supplementary material 4. Results of the selection of substitution model for redefined partitions. File format: TXT.

Electronic supplementary material 5. Measurements of animals and eggs. File format: XLSX.

Electronic supplementary material 6. Matrices of *p*-distances for *Tenuibiotus* species. File format: XLSX.

All these materials are available from: <https://doi.org/10.31610/zsr/2024.33.1.28>

not provide any photographs of the specimens. Upon reexamination of the type material, we can conclude that areolation on the egg surface in *T. bondavallii* is absent (Fig. 8d).

Acknowledgements

We would like to thank Yelisei Mesentsev (St Petersburg State University) for collecting the sample used in this study. We are grateful to Giovanni Pilato and Maria Grazia Binda (Catania University), to Roberto Bertolani and Roberto Guidetti (University of Modena and Reggio Emilia) for providing the slides and photographs of the type material for several *Tenuibiotus* species examined in this work. This study was carried out with the use of equipment of the Core Facilities Centres ‘Centre for Molecular and Cell Technologies’ and ‘Centre for Culture Collection of Microorganisms’ of St Petersburg State University. The work was supported by the State scientific programme ‘Taxonomy, biodiversity and ecology of invertebrates from Russian and adjacent waters of World Ocean, continental water bodies and damped areas’ No. 122031100275-4.

References

- Beasley C. & Miller W. 2012. Additional Tardigrades from Hubei Providence, China, with the description of *Doryphoribius barbarae* sp. nov. (Eutardigrada: Parachela: Hypsibiidae). *Zootaxa*, **3170**: 55–63. <https://doi.org/10.11646/zootaxa.3170.1.5>
- Bertolani R., Biserov V., Rebecchi L. & Cesari M. 2011a. Taxonomy and biogeography of tardigrades using an integrated approach: new results on species of the *Macrobiotus hufelandi* group. *Invertebrate Zoology*, **8**(1): 23–36. <https://doi.org/10.15298/invertzool.08.1.05>
- Bertolani R., Rebecchi L., Giovannini I. & Cesari M. 2011b. DNA barcoding and integrative taxonomy of *Macrobiotus hufelandi* C.A.S. Schultz 1834, the first tardigrade species to be described, and some related species. *Zootaxa*, **2997**: 19–36. <https://doi.org/10.11646/zootaxa.2997.1.2>
- Bertolani R., Guidetti R., Marchioro T., Altiero T., Rebecchi L. & Cesari M. 2014. Phylogeny of Eutardigrada: New molecular data and their morphological support lead to the identification of new evolutionary lineages. *Molecular Phylogenetics and Evolution*, **76**: 110–126. <https://doi.org/10.1016/j.ympev.2014.03.006>
- Binda M.G. & Pilato G. 1972. Tardigradi muscicoli di Sicilia. (IV Nota). *Bollettino delle sedute dell'Accademia Gioenia di Scienze Naturali, Catania, Serie 4*, **11**: 47–60.
- Biserov V. 1996. Tardigrades of the Taimyr Peninsula with descriptions of two new species. *Zoological Journal of the Linnean Society*, **116**(1–2): 215–237. <https://doi.org/10.1006/zjls.1996.0018>

- Biserov V.** 1999. Tardigrada of Turkmenistan, with description of three new species. *Zoologischer Anzeiger*, **238**: 157–167.
- Degma P. & Guidetti R.** 2023. *Actual checklist of Tardigrada species. 42th Edition* [online]. Università degli studi di Modena e Reggio Emilia: IRIS Unimore. <https://iris.unimore.it/retrieve/bf8e14a4-625f-4cdd-8100-347e5cbc5f63/Actual%20checklist%20of%20Tardigrada%2042th%20Edition%2009-01-23.pdf> [updated 9 January 2023; viewed 15 June 2023]. https://doi.org/10.25431/11380_1178608
- Dudichev A.L. & Biserov V.I.** 2000. Tardigrada from Iturup and Paramushir islands (the Kuril Islands). *Zoologicheskii Zhurnal*, **79**(7): 771–778. (In Russian).
- Gąsiorek P., Stec D., Morek W., Zawierucha K., Kaczmarek Ł., Lachowska-Cierlik D. & Michalczyk Ł.** 2016. An integrative revision of Mesocrista Pilato, 1987 (Tardigrada: Eutardigrada: Hypsibiidae). *Journal of natural History*, **50**(45–46): 2803–2828. <https://doi.org/10.1080/00222933.2016.1234654>
- Gąsiorek P., Stec D., Morek W. & Michalczyk Ł.** 2018. An integrative redescription of Hypsibius dujardini (Doyère, 1840), the nominal taxon for Hypsibioidea (Tardigrada: Eutardigrada). *Zootaxa*, **4415**(1): 45–75. <https://doi.org/10.11646/zootaxa.4415.1.2>
- Gąsiorek P., Morek W., Stec D., Blagden B. & Michalczyk Ł.** 2019. Revisiting Calohypsibiidae and Microhypsibiidae: Fractonotus Pilato, 1998 and its phylogenetic position within Isohypsibiidae (Eutardigrada: Parachela). *Zoosystema*, **41**(1): 71–89. <https://doi.org/10.5252/zoosystema2019v41a6>
- Gouy M., Guindon S. & Gascuel O.** 2010. SeaView version 4: A multiplatform graphical user interface for sequence alignment and phylogenetic tree building. *Molecular Biology and Evolution*, **27**: 221–224. <https://doi.org/10.1093/molbev/msp259>
- Guidetti R., Cesari M., Bertolani R., Altiero T. & Rebecchi L.** 2019. High diversity in species, reproductive modes and distribution within the Paramacrobiotus richtersi complex (Eutardigrada, Macrobiotidae). *Zoological Letters*, **5**: 1. <https://doi.org/10.1186/s40851-018-0113-z>
- Guil N. & Giribet G.** 2012. A comprehensive molecular phylogeny of tardigrades – adding genes and taxa to a poorly resolved phylum-level phylogeny. *Cladistics*, **28**: 21–49. <https://doi.org/10.1111/j.1096-0031.2011.00364.x>
- Guil N., Guidetti R. & Machordom A.** 2007. Observations on the “tenuis group” (Eutardigrada, Macrobiotidae) and description of a new Macrobiotus species. *Journal of natural History*, **41**(41–44): 2741–2755. <https://doi.org/10.1080/00222930701742637>
- Guil N., Jørgensen A. & Kristensen R.** 2019. An upgraded comprehensive multilocus phylogeny of the Tardigrada tree of life. *Zoologica Scripta*, **48**: 120–137. <https://doi.org/10.1111/zsc.12321>
- Johansson C., Miller W.R., Linder E.T., Adams B.J. & Boreliz-Alvarado E.** 2013. Tardigrades of Alaska: distribution patterns, diversity and species richness. *Polar Research*, **32**: 1–11. <https://doi.org/10.3402/polar.v32i0.18793>
- Jørgensen A., Faurby S., Hansen J.G., Møbjerg N. & Kristensen R.M.** 2010. Molecular phylogeny of Arthrotardigrada (Tardigrada). *Molecular Phylogenetics and Evolution*, **54**: 1006–1015. <https://doi.org/10.1016/j.ympev.2009.10.006>
- Jørgensen A., Møbjerg N. & Kristensen R.M.** 2011. Phylogeny and evolution of the Echiniscoidea (Echiniscoidea, Tardigrada) – an investigation of the congruence between molecules and morphology. *Journal of zoological Systematics and evolutionary Research*, **49**: 6–16. <https://doi.org/10.1111/j.1439-0469.2010.00592.x>
- Kaczmarek Ł. & Michalczyk Ł.** 2017. The Macrobiotus hufelandi group (Tardigrada) revisited. *Zootaxa*, **4363**(1): 101–123. <https://doi.org/10.11646/zootaxa.4363.1.4>
- Kaczmarek Ł., Cytan J., Zawierucha K., Diduszko D. & Michalczyk Ł.** 2014. Tardigrades from Peru (South America), with descriptions of three new species of Parachela. *Zootaxa*, **3790**(2): 357–379. <http://doi.org/10.11646/zootaxa.3790.2.5>
- Kaczmarek Ł., Michalczyk Ł. & McInnes S.J.** 2016. Annotated zoogeography of non-marine Tardigrada. Part III: North America and Greenland. *Zootaxa*, **4203**(1): 1–249. <https://doi.org/10.11646/zootaxa.4203.1.1>
- Kalyaanamoorthy S., Minh B., Wong T., von Haeseler A. & Jermini L.S.** 2017. ModelFinder: fast model selection for accurate phylogenetic estimates. *Nature Methods*, **14**: 587–589. <https://doi.org/10.1038/nmeth.4285>
- Katoh K., Misawa K., Kuma K. & Miyata T.** 2002. MAFFT: a novel method for rapid multiple sequence alignment based on fast Fourier transform. *Nucleic Acids Research*, **30**(14): 3059–3066. <https://doi.org/10.1093/nar/gkf436>
- Kayastha P., Stec D., Sługocki Ł., Gawlak M., Mioduchowska M. & Kaczmarek Ł.** 2023. Integrative taxonomy reveals new, widely distributed tardigrade species of the genus Paramacrobiotus (Eutardigrada: Macrobiotidae). *Scientific Reports*, **13**: 2196. <https://doi.org/10.1038/s41598-023-28714-w>

- Kiosya Y., Pogwizd J., Matsko Y., Vecchi M. & Stec D.** 2021. Phylogenetic position of two Macrobiotus species with a revisional note on Macrobiotus sottilei Pilato, Kiosya, Lisi & Sabella, 2012 (Tardigrada: Eutardigrada: Macrobiotidae). *Zootaxa*, **4933**(1): 113–135. <https://doi.org/10.11646/zootaxa.4933.1.5>
- Larsson A.** 2014. AliView: a fast and lightweight alignment viewer and editor for large data sets. *Bioinformatics*, **30**(22): 3276–3278. <http://doi.org/10.1093/bioinformatics/btu531>
- Manicardi G.C.** 1989. Two new species of soil moss eutardigrades (Tardigrada) from Canada. *Canadian Journal of Zoology*, **67**(9): 2282–2285. <https://doi.org/10.1139/z89-321>
- Maucci W.** 1978. Tardigradi muscicoli della Turchia (Terzo contributo). *Bollettino del Museo Civico di Storia Naturale di Verona*, **5**: 111–140.
- Maucci W.** 1982. Sulla presenza in Italia di Cornechiniscus holmeni (Petersen, 1951) e descrizione di Macrobiotus hyperonyx sp. nov. (Tardigrada). *Bollettino del Museo Civico di Storia Naturale di Verona*, **9**: 175–179.
- Maucci W.** 1987. A contribution to the knowledge of the North American Tardigrada with emphasis on the fauna of Yellowstone National Park (Wyoming). In: **Bertolani R.** (Ed.). *Biology of tardigrades: Proceedings of the 4th International Symposium on the Tardigrada, Modena, September 3–5, 1985*: 187–210. Modena: Mucchi.
- Maucci W.** 1988. Tardigradi della Mongolia esterna, con descrizione di Macrobiotus mongolicus sp. nov. *Bollettino del Museo Civico di Storia Naturale di Verona*, **14**: 339–349.
- McInnes S.J.** 1994. Zoogeographic distribution of terrestrial/freshwater tardigrades from current literature. *Journal of natural History*, **28**(2): 257–352. <https://doi.org/10.1080/00222939400770131>
- Michalczyk Ł. & Kaczmarek Ł.** 2003. A description of the new tardigrade Macrobiotus reinhardti (Eutardigrada: Macrobiotidae, harmsworthi group) with some remarks on the oral cavity armature within the genus Macrobiotus Schultze. *Zootaxa*, **331**(1): 1–24. <https://doi.org/10.11646/zootaxa.331.1.1>
- Michalczyk Ł. & Kaczmarek Ł.** 2013. The Tardigrada Register: a comprehensive online data repository for tardigrade taxonomy. *Journal of Limnology*, **72**(S1): e22. <https://doi.org/10.4081/jlimnol.2013.s1.e22>
- Miller M. A., Pfeiffer W. & Schwartz T.** 2010. Creating the CIPRES Science Gateway for inference of large phylogenetic trees. *Gateway computing environments workshop (GCE)*: 1–8. <https://doi.org/10.1109/GCE.2010.5676129>
- Minh B., Hahn M. & Lanfear R.** 2020. New methods to calculate concordance factors for phylogenomic datasets. *Molecular Biology and Evolution*, **37**(9): 2727–2733. <https://doi.org/10.1093/molbev/msaa106>
- Morek W., Stec D., Gąsiorek P., O. Schill R., Kaczmarek Ł. & Michalczyk Ł.** 2016. An experimental test of eutardigrade preparation methods for light microscopy. *Zoological Journal of the Linnean Society*, **178**(4): 785–793. <https://doi.org/10.1111/zoj.12457>
- Pilato G.** 1977. Macrobiotus willardi, a new species of Tardigrada from Canada. *Canadian Journal of Zoology*, **55**: 628–630. <https://doi.org/10.1139/z77-080>
- Pilato G.** 1981. Analisi di nuovi caratteri nello studio degli Eutardigradi. *Animalia*, **8**(1/3): 51–57.
- Pilato G. & Binda M.G.** 2010. Definition of families, subfamilies, genera and subgenera of the Eutardigrada, and keys to their identification. *Zootaxa*, **2404**(1): 1–54. <https://doi.org/10.11646/zootaxa.2404.1.1>
- Pilato G., Kiosya Y., Lisi O., Inshina V. & Biserov V.** 2011. Annotated list of Tardigrada records from Ukraine with the description of three new species. *Zootaxa*, **3123**: 1–31. <https://doi.org/10.11646/zootaxa.3123.1.1>
- Pilato G. & Lisi O.** 2011. Tenuibiotus, a new genus of Macrobiotidae (Eutardigrada). *Zootaxa*, **2761**: 34–40. <https://doi.org/10.11646/zootaxa.2761.1.2>
- Pleijel F., Jondelius U., Norlinder E., Nygren A., Oxelman B., Schander C., Sundberg P. & Thollesson M.** 2008. Phylogenies without roots? A plea for the use of vouchers in molecular phylogenetic studies. *Molecular Phylogenetics and Evolution*, **48**(1): 369–371. <https://doi.org/10.1016/j.ympev.2008.03.024>
- Rambaut A., Drummond A.J., Xie D., Baele G. & Suchard M.A.** 2018. Posterior summarisation in Bayesian phylogenetics using Tracer 1.7. *Systematic Biology*, **67**(5): 901–904. <https://doi.org/10.1093/sysbio/syy032>
- Ronquist F. & Huelsenbeck J.P.** 2003. MrBayes 3: Bayesian phylogenetic inference under mixed models. *Bioinformatics*, **19**(12): 1572–1574. <https://doi.org/10.1093/bioinformatics/btg180>
- Stec D., Gąsiorek P., Morek W., Kosztyła P., Zawierucha K., Michno K., Kaczmarek Ł., Prokop Z.M. & Michalczyk Ł.** 2016. Estimating optimal sample size for tardigrade morphometry. *Zoological Journal of the Linnean Society*, **178**: 776–784. <https://doi.org/10.1111/zoj.12404>
- Stec D. & Morek W.** 2022. Reaching the monophyly: re-evaluation of the enigmatic species Tenuibiotus hyperonyx (Maucci, 1983) and the genus Tenuibi-

- otus (Eutardigrada). *Animals*, **12**: 404. <https://doi.org/10.3390/ani12030404>
- Stec D., Morek W., Gašiorek P. & Michalczyk Ł.** 2018. Unmasking hidden species diversity within the Ramazzottius oberhaeuseri complex, with an integrative redescription of the nominal species for the family Ramazzottiidae (Tardigrada: Eutardigrada: Parachela). *Systematics and Biodiversity*, **16**(4): 357–376. <https://doi.org/10.1080/14772000.2018.1424267>
- Stec D., Tumanov D. & Kristensen R.M.** 2020. Integrative taxonomy identifies two new tardigrade species (Eutardigrada: Macrobiotidae) from Greenland. *European Journal of Taxonomy*, **614**: 1–40. <https://doi.org/10.5852/ejt.2020.614>
- Stec D., Vecchi M., Calhim S. & Michalczyk Ł.** 2021a. New multilocus phylogeny reorganises the family Macrobiotidae (Eutardigrada) and unveils complex morphological evolution of the Macrobiotus hufelandi group. *Molecular Phylogenetics and Evolution*, **160**: 106987. <https://doi.org/10.1016/j.ympev.2020.106987>
- Stec D., Vecchi M., Dudziak M., Bartels P.J., Calhim S. & Michalczyk Ł.** 2021b. Integrative taxonomy resolves species identities within the Macrobiotus pallarii complex (Eutardigrada: Macrobiotidae). *Zoological Letters*, **7**: 9. <https://doi.org/10.1186/s40851-021-00176-w>
- Stec D., Vončina K., Kristensen R.M. & Michalczyk Ł.** 2022. The Macrobiotus ariekammensis species complex provides evidence for parallel evolution of claw elongation in macrobiotid tardigrades. *Zoological Journal of the Linnean Society*, **195**(4): 1067–1099. <https://doi.org/10.1093/zoolinnea/zlab101>
- Tamura K., Stecher G. & Kumar S.** 2021. MEGA11: Molecular Evolutionary Genetics Analysis Version 11. *Molecular Biology and Evolution*, **38**(7): 3022–3027. <https://doi.org/10.1093/molbev/msab120>
- Tumanov D.V.** 2005. Two new species of Macrobiotus (Eutardigrada, Macrobiotidae) from Tien Shan (Kirghizia), with notes on the Macrobiotus tenuis group. *Zootaxa*, **1043**: 3–46. <https://doi.org/10.11646/zootaxa.1043.1.3>
- Tumanov D.V.** 2007. Three new species of Macrobiotus (Eutardigrada, Macrobiotidae, tenuis-group) from Tien Shan (Kirghizia) and Spitsbergen. *Journal of Limnology*, **66**(Supplement): 40–48. <https://doi.org/10.4081/jlimnol.2007.s1.40>
- Tumanov D.V.** 2018. Hypsibius vaskelae, a new species of Tardigrada (Eutardigrada, Hypsibiidae) from Russia. *Zootaxa*, **4399**(3): 434–442. <https://doi.org/10.11646/zootaxa.4399.3.12>
- Tumanov D.V.** 2020. Integrative redescription of Hypsibius pallidoides Pilato et al., 2011 (Eutardigrada: Hypsibioidea) with the erection of a new genus and discussion on the phylogeny of Hypsibiidae. *European Journal of Taxonomy*, **681**: 1–37. <https://doi.org/10.5852/ejt.2020.681>
- Węglarska B.** 1965. Die Tardigraden (Tardigrada) Spitzbergens. *Acta zoologica Cracoviensia*, **11**: 43–51.
- Zawierucha K., Kolicka M. & Kaczmarek Ł.** 2016. Re-description of the Arctic tardigrade Tenuibiotus voronkovi (Tumanov, 2007) (Eutardigrada; Macrobiotidae), with the first molecular data for the genus. *Zootaxa*, **4196**(4): 498–510. <http://doi.org/10.11646/zootaxa.4196.4.2>

Received 26 July 2023 / Accepted 22 April 2024. Editorial responsibility: A.A. Przhiboro